Self-Phase-Matched High Harmonic Generation

Gabriel Tempea, Michael Geissler, Matthias Schnürer, and Thomas Brabec*
Institut für Photonik, Technische Universität Wien, Gusshausstrasse 27/387, A-1040 Wien, Austria
(Received 6 May 1999)

Our theoretical analysis reveals that tunnel ionization significantly modifies the electric field of few-cycle laser pulses within a single oscillation period. This subcycle self-modulation is predicted to result in phase matching, making high harmonic generation in the x-ray regime possible for the first time. Such a radiation source opens novel possibilities in the investigation of matter with x-ray techniques, such as time resolved x-ray diffraction and absorption.

PACS numbers: 42.50.Hz, 32.80.Rm, 42.65.Ky

High harmonic generation (HHG) in noble gases [1] is a promising source for the generation of coherent extreme-ultraviolet (XUV) radiation; however, the efficiency is still too low for many important applications. In the XUV and x-ray range, free-electron-induced dephasing presents the main limitation [2] confining HHG to photon energies below 0.5 keV [3,4]. Therefore, in order to realize shorter wavelengths and higher efficiencies, phase matching schemes [5] for the compensation of dephasing are required.

Theoretical treatment of phase matching usually relies on the adiabatic approximation [5], whereby the change of the free electron density during one optical cycle may be neglected. Under this assumption the harmonic phase grows linearly with propagation distance. In our theoretical analysis a novel phase matching mechanism is identified that works predominantly for few-cycle, high-intensity laser pulses and for wavelengths in the XUV and x-ray regime. In this so-called nonadiabatic parameter regime the ionization rate becomes comparable to the center frequency of the laser pulse leading to a significant change of the free electron density over one optical cycle. The rapidly varying ionization front causes subcycle changes of the laser electric field, which give rise to an additional (nonadiabatic) contribution to the harmonic phase growing nonlinearly with the interaction length. The nonadiabatic and adiabatic phase contributions are opposite in sign and can compensate resulting in phase-matched growth. We have dubbed this mechanism nonadiabatic self-phase matching (NSPM). NSPM does not work close to the single atom cutoff, where previous investigations of HHG with few-cycle pulses were performed [6]. This is because plasma dispersion reduces the laser intensity below the intensity necessary for HHG in the cutoff region, before NSPM starts to play a role. Finally, our calculations predict that NSPM enhances HHG above 1 keV by 4 orders of magnitude, thus making for the first time HHG in the soft x-ray regime possible.

For the analysis of HHG with few-cycle laser pulses the theoretical model introduced in Ref. [7] is used. HHG is modeled by a solution of the coupled propagation equations for the fundamental (E_l) and for the harmonic (E_h) fields in one space dimension. The atomic dipole moment, which is the source term for HHG, is determined by a generalized Lewenstein model [7,8] which also accounts for nonadiabatic effects [6]. To test our model, in Fig. 1 numerical results are compared to experimental data obtained from the setup described in Ref. [4]. For these parameters the shortest harmonics so far were generated. Excellent agreement between experiment and theory is obtained corroborating the reliability of our model.

Plot (*a*) in Fig. 1 reveals a rapid decrease of the harmonic spectrum with increasing order. The wavelength dependence comes from the fact that the maximum spectral intensity of the *N*th harmonic depends quadratically on the coherence length $L = 2\pi c\omega_0/N\omega_p^2(\tau) \propto 1/Nn(\tau)$ [6]. The strong increase of the free electron density $n(\tau)$ with increasing harmonic order is mainly responsible for

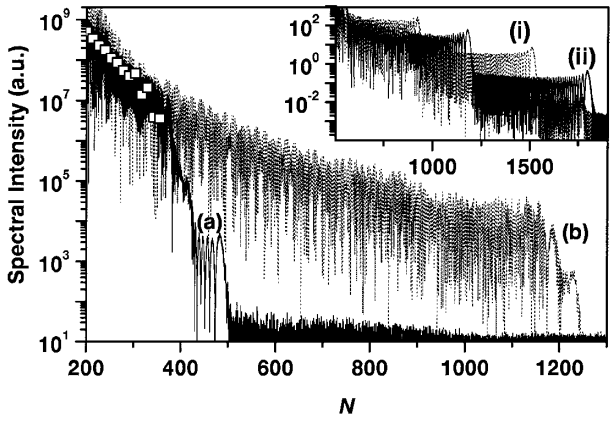

FIG. 1. The spectral intensity of harmonic radiation generated after propagation of 125 μm in He (500 Torr) versus harmonic order for a Ti:sapphire pulse with $\lambda_0 \approx 0.8$ μm, $\tau_f = 5$ fs, $I_0 = 4 \times 10^{15}$ W/cm^2, and 0.3 mJ pulse energy at a repetition rate of 1 kHz [plot (*a*), full line], and $I_0 = 1.5 \times 10^{16}$ W/cm^2 [plot (*b*), dotted line]. The open squares denote the experimentally measured values for the parameters of plot (*a*). A constant parameter was introduced in the calculations to obtain optimum agreement between experiment and theory. The inset shows the single atom dipole spectrum for the parameters of (*b*) after propagation distances of 0 μm [(i) dotted line] and 15 μm [(ii) full line)].

the rapid drop of the harmonic spectrum. Here, $\omega_p^2(\tau) = 4\pi n(\tau)e^2/m$ is the plasma frequency squared at time τ, ω_0 is the center circular frequency of the laser pulse, c is the vacuum velocity of light, and e and m are the electron charge and mass, respectively.

The harmonic spectrum (b) in Fig. 1 corresponds to a higher peak intensity $I_0 = 1.5 \times 10^{16}$ W/cm^2. In contrast to plot (a), the decrease of harmonic intensity for $N > 300$ is significantly reduced, and the spectrum remains nearly constant at the high energy end indicating that the coherence length L is no longer a correct measure of the harmonic growth. This anomalous behavior originates from NSPM which will be explained below in detail. A remarkable consequence of NSPM is that harmonics up to an order $N = 1200$ are generated, corresponding to a photon energy close to 2 keV. The efficiency of HHG in the keV regime can be estimated from a comparison of our calculations to experiments. Estimation of the absolute photon number for the experimental data in Fig. 1 yields that $\approx 10^7$ photon/s were generated at the 300th harmonic in a 5% bandwidth [4]. Comparison of the energies contained in a 5% bandwidth of spectra (a)/(b) at $N = 300/1000$ in Fig. 1 yields a ratio of $\approx 10^{-3}$ and reveals that $\approx 10^4$ photons/s in a 5% bandwidth at 1.5 keV can be generated [9].

In contrast to the cutoff of the propagated signal, the single atom dipole cutoff in the inset of Fig. 1 exhibits several cutoffs at $N = 1800$, $N = 1500$, and $N = 900$ corresponding to electron trajectories returning to the nucleus at the pulse peak, one half cycle before and two half cycles before the pulse peak, respectively. The lowest cutoff corresponds to an intensity of 8×10^{15} W/cm^2, where 98% of the first electron of He is ionized. At such high laser intensities the ionization rate is so strong that in spite of ground state depletion HHG beyond the first cutoff can take place, however, with a rapid drop of efficiency between subsequent half cycles. The single atom cutoffs undergo significant shifts during propagation that arise from changes of the laser pulse due to plasma dispersion and nonlinearity. After 15 μm propagation distance the cutoff is shifted from $N = 1500$ to $N = 1200$. For $N = 1250$ (see Fig. 4) NSPM does not take place within the first 15 μm explaining the different cutoffs found for the single atom and for the propagated signal.

In Fig. 2 the growth of energy contained in the spectral window between the 950th and the 1000th harmonic is plotted versus interaction length for the parameters of spectrum (b) in Fig. 1. The inset shows the evolution of the harmonic signal over the first μm. The harmonic signal grows over the coherence length $L \approx 0.1$ μm, and oscillates for $\xi > L$ between a maximum and a minimum value. For $\xi \gg L$, NSPM sets in and the harmonic signal exhibits a steplike increase which enhances the energy converted into harmonic radiation by 4 orders of magnitude. The length over which NSPM occurs is denoted by L_s. During the first step between 4 and 7 μm we find

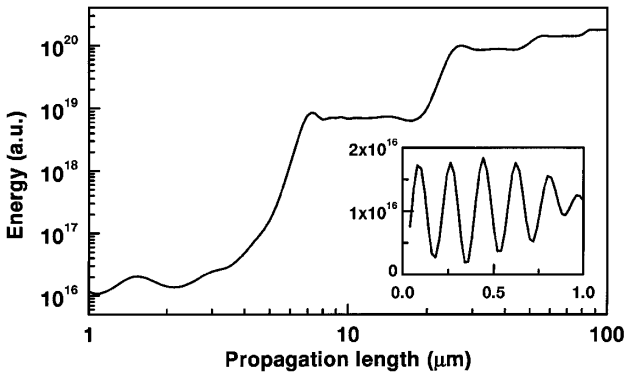

FIG. 2. Energy of the harmonic signal between $N = 950$ and $N = 1000$ versus propagation distance for the parameters of graph (b) in Fig. 1. The inset shows the growth of the harmonic over the first μm.

$L_s/L \approx 30$, and the enhancement $(L_s/L)^2 \approx 900$ agrees well with the observed signal growth by 3 orders of magnitude, indicating the coherent nature of the emitted radiation. Inspection of the temporal profile of the harmonic spectrum between $N = 950$ and 1000 shows that during the first 10 μm a single pulse with a duration of 40 attoseconds (40×10^{-18} s) grows. At longer interaction distances the harmonic signal grows at other positions of the laser pulse which results in the generation of an attosecond pulse train extending over 5 fs.

The calculation in Fig. 2 was repeated for several other spectral windows (i), peak intensities (ii), pulse durations (iii), and noble gases (iv), from which the following general conclusions can be drawn.

(i) As explained above, NSPM does not work close to the single atom cutoff. Away from the cutoff, where significant ionization takes place, we find that the NSPM induced enhancement, determined by the ratio L_s/L, increases for higher harmonic orders. The reason for this behavior is that L decreases, whereas our calculations show that L_s changes only weakly with increasing N. For example, the harmonic range between $N = 190$ and 210 in Fig. 1(b) experiences an NSPM induced growth by 1 order of magnitude. The strongest increase in harmonic efficiency (4–5 orders of magnitude) is observed in the spectral range between $N = 800$ and $N = 1200$ in Fig. 1. (ii) The NSPM induced gain is strongest for peak intensities larger than the saturation intensity of ionization, at which most of the first electron of helium (98%) is ionized. In this parameter range the harmonic yield is found to be rather insensitive to variations of the peak intensity demonstrating that NSPM can take place in a significant volume of the fundamental beam. (iii) The effect of NSPM is strongest for few-cycle laser pulses and decreases rapidly with increasing pulse duration. For a 20-fs pulse with a peak intensity of 1.5×10^{16} W/cm^2 [for the other parameters see graph (b) in Fig. 1], the cutoff of the propagated signal is found to be around $N = 500$. The signal generated by the 20 fs pulse between $N = 390$ and 410 is

enhanced due to NSPM by a factor less than 10. (iv) Calculations for noble gases with lower ionization potentials yield a qualitatively similar behavior as found in He demonstrating that NSPM does not depend on a particular atomic species. This opens the possibility to shift the spectral window, where NSPM is most pronounced, to lower harmonic orders by using a gas with a lower ionization potential.

In the following, the mechanism for NSPM is identified by investigating the phase growth ϕ_N of a selected harmonic N. Phase-matched growth occurs as long as the harmonic phase does not change, i.e., $d\phi_N/d\xi \approx 0$. A schematic of the laser and harmonic fields generated at two propagation distances ξ_1 and $\xi_2 = \xi_1 + \Delta\xi$ in a frame moving at vacuum light velocity is depicted in Fig. 3. According to the quasiclassical interpretation of HHG [8], the harmonic N is generated by an electron that is born by tunnel ionization at a time τ_b and that recombines to the ground state at an instant τ_r. The evolution of the electron between τ_b and τ_r is determined by the laser electric field. The phase of the harmonic is obtained from a Fourier transform of the atomic dipole moment, as given by Eq. (4) in Ref. [7], which yields

$$\phi_N = S(\tau_b(\xi), \tau_r(\xi)) - N\omega_0\tau_r(\xi). \qquad (1)$$

The quasiclassical action S [8,10] is determined by the phase change of the electron wave packet (responsible for generation of the Nth harmonic) during propagation in the laser field between τ_b and τ_r.

The primary change in ϕ_N results from a shift of τ_r in Eq. (1). The laser field experiences a blueshift of the frequency in the presence of ionization [11]. The resulting phase shift grows linearly with propagation distance, $\phi_l(\xi) = \omega_p^2(\tau)\xi/2c\omega_0$ [5,6]. In the frame propagating at the vacuum speed of light, which is comoving with the harmonic wave, this phase change shifts the time τ_r, at which the harmonic is generated as $\tau_r(\xi_2) = \tau_r(\xi_1) + \phi_l(\Delta\xi)/\omega_0$. By virtue of (1) the shift of τ_r causes a change of the harmonic phase.

In the adiabatic limit of many-cycle pulses the change of free electron density during one laser cycle is negligible, hence $\Delta n = n(\tau_r) - n(\tau_b) \approx 0$. This implies that τ_r and τ_b are shifted by the same amount with increasing propagation distance $\Delta\xi$ and that the laser electric field experienced by the electron between τ_r and τ_b remains unchanged, as illustrated in Fig. 3(a). As a consequence, the quasiclassical action S remains constant. Inserting the resulting phase change into the condition $\phi_N(\xi_2) - \phi_N(\xi_1) = N\phi_l = \pi$ yields the coherence length L as given above.

The nonadiabatic behavior originates from a strong subcycle variation of the free electron density Δn and from the resulting subcycle changes of the laser electric field. As a consequence, the trajectories of the freed electrons are governed by slightly different electric field evolutions (in time) at different positions along the propagation direction, as illustrated in Fig. 3(b). Therefore, the quasiclassical action S changes with ξ. The nonadiabatic $[S(\xi_2) - S(\xi_1)]$ and the adiabatic phase changes are opposite in sign reducing growth of the harmonic phase ϕ_N. For few-cycle laser pulses the nonadiabatic contribution can become strong enough to compensate the adiabatic change of the harmonic phase giving rise to NSPM; see Fig. 4.

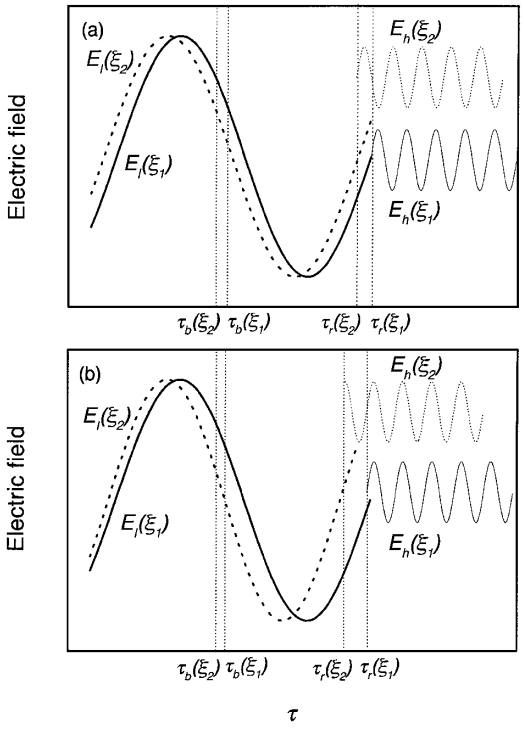

FIG. 3. Schematic of the fundamental field E_l and of the harmonic field E_h (generated) at ξ_1 (full lines) and at ξ_2 (dotted lines) in the limits of (a) adiabatic evolution (many-cycle laser pulse) and (b) nonadiabatic evolution (few-cycle laser pulse). The times τ_b and τ_r are the birth and recombination times of the electron that generates a particular harmonic N. The electric fields are plotted in a retarded frame propagating with vacuum light velocity, in which the harmonic field does not change with propagation. The phase difference of harmonics generated at different propagation distances ξ_1 and ξ_2 comes from the ionization induced modification of the fundamental field. In the adiabatic limit (a), the change in free electrons $\Delta n = n(\tau_r) - n(\tau_b) \approx 0$ and the laser field experiences a phase shift that is approximately constant in the time interval between τ_b and τ_r. As the electrons at ξ_1 and ξ_2 experience the same electric field, the phases of the harmonics generated at $\tau_r(\xi_1)$ and at $\tau_r(\xi_2)$ are equal $[S(\xi_2) - S(\xi_1) \approx 0]$. The adiabatic phase mismatch is introduced by a shift of the time $\tau_r(\xi_2) - \tau_r(\xi_1)$ at which the harmonic signal is generated. The nonadiabatic behavior (b) originates from a rapidly changing ionization profile ($\Delta n \neq 0$) causing a subcycle variation of the laser electric field. As a consequence, the trajectories of the freed electrons are governed by slightly different electric fields. Therefore, the phases of the harmonic $E_h(\xi_1)$ generated at $\tau_r(\xi_1)$ and of $E_h(\xi_2)$ at $\tau_r(\xi_2)$ are no longer equal. The resulting nonadiabatic harmonic phase change $[S(\xi_2) - S(\xi_1) \neq 0]$ is opposite in sign to the adiabatic phase contribution and can cancel it (b) leading to phase-matched growth.

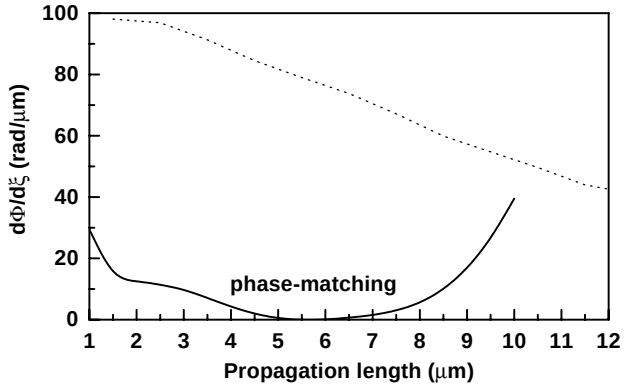

FIG. 4. The evolution of the phase change of the harmonics $N = 975$ (full line) and $N = 1250$ (dotted line) versus propagation distance for the parameters of Fig. 2. The phase change of the harmonic order $N = 975$ is zero exactly at the position at which NSPM takes place in Fig. 2. For the harmonic order $N = 1250$, NSPM does not take place within the first 15 μm. For distances larger than 15 μm, NSPM cannot take place, as the single atom cutoff is shifted below $N = 1250$; see the inset of Fig. 1. This explains the difference between the cutoff positions of the single atom dipole response and of the propagated harmonic spectrum in Fig. 1.

Between 4 and 7 μm, $d\phi_N/d\xi \approx 0$ (for $N = 975$), and NSPM takes place in accordance with Fig. 2.

Finally, our model of HHG does not take account of the $\mathbf{v} \times \mathbf{B}$ (Lorentz) force that becomes significant at high laser intensities. Here, $\mathbf{v}$ is the velocity of the electron and $\mathbf{B}$ is the magnetic field of the laser pulse. The Lorentz force shifts the electron trajectory during continuum propagation in the direction of the laser wave vector [12]. The influence of this contribution on HHG can be determined by a semiclassical estimate. We assume that the electron is born at zero velocity. Then a solution of the classical (relativistic) equations of motion for the 975th harmonic in Fig. 1 yields an offset $x_l \approx 1$ nm, when the electron returns to the nucleus. This shift must be compared to the transversal width of the returning electron wave function, $x_r = v_b(\tau_r - \tau_b)$, in order to determine the influence on HHG. Here, $\tau_r - \tau_b \approx 2.2$ fs is the interval between birth and return time of the electron, and v_b is the width of the velocity distribution of the electron wave packet at its birth. To estimate a lower limit for x_r, it is assumed that the initial spatial distribution of the electron wave packet at its birth is equal to the Bohr radius, $x_b = 5.3 \times 10^{-9}$ cm. By virtue of the uncertainty relation ($x_b v_b \geq \hbar/2m$) we obtain the initial transversal velocity spread $v_b \approx 10^8$ cm/s and from that $x_r \approx 2.5$ nm. As $x_r > x_l$, neglect of the Lorentz force in our calculations is justified.

The authors gratefully acknowledge the support of Professor A. J. Schmidt, and invaluable discussions with F. Krausz, Ch. Spielmann, M. Murnane, and H. Kapteyn. This work was supported by the Austrian Science Fund, Grant No. P12631-PHY and special research program F016, and by the Austrian Nationalbank, Grant No. 7178.

*Electronic address: brabec@tuwien.ac.at

[1] A. McPherson *et al.*, J. Opt. Soc. Am. B **4**, 595 (1987); A. L'Huillier and P. Balcou, Phys. Rev. Lett. **70**, 774 (1993); J. J. Macklin, J. D. Kmetec, and C. L. Gordon III, Phys. Rev. Lett. **70**, 766 (1993).

[2] M. Schnürer *et al.*, Phys. Rev. Lett. **83**, 722 (1999).

[3] Z. Chang, A. Rundquist, H. Wang, M. M. Murnane, and H. C. Kapteyn, Phys. Rev. Lett. **79**, 2967 (1997).

[4] Ch. Spielmann *et al.*, Science **278**, 661 (1997); M. Schnürer *et al.*, Phys. Rev. Lett. **80**, 3236 (1998).

[5] H. M. Milchberg, C. G. Durfee III, and T. J. McIlrath, Phys. Rev. Lett. **75**, 2494 (1995); P. L. Shkolnikov, A. E. Kaplan, and A. Lago, J. Opt. Soc. Am. B **13**, 412 (1996); J. Peatross, S. Voronov, and I. Prokopovich, Opt. Express **1**, 114 (1997); I. P. Christov, H. C. Kapteyn, and M. M. Murnane, Opt. Express **3**, 360 (1998); A. Rundquist *et al.*, Science **280**, 1412 (1998); H. R. Lange *et al.*, Phys. Rev. Lett. **81**, 1611 (1998); Y. Tamaki, J. Itatani, Y. Nagata, M. Obara, and K. Midorikawa, Phys. Rev. Lett. **82**, 1422 (1999).

[6] C. Kan, N. H. Burnett, C. E. Capjack, and R. Rankin, Phys. Rev. Lett. **79**, 2971 (1997); P. Saliéres, P. Antoine, A. de Bohan, and M. Lewenstein, Phys. Rev. Lett. **81**, 5544 (1998); I. P. Christov, M. M. Murnane, and H. C. Kapteyn, Phys. Rev. A **57**, R2285 (1998).

[7] M. Geissler, G. Tempea, and T. Brabec, "Phase matched high harmonic generation: the role of nonadiabatic effects" (to be published); G. Tempea, M. Geissler, and T. Brabec, J. Opt. Soc. Am. B **16**, 669 (1999).

[8] M. Lewenstein *et al.*, Phys. Rev. A **49**, 2117 (1994).

[9] At peak intensities of $\approx 10^{16}$ W/cm^2 a clean (leading) pulse front is required in order to avoid preionization, which can suppress NSPM.

[10] Using the notation of Ref. [7] the quasiclassical action is given by $S = (1/\hbar)\int_{\tau_b}^{\tau_r} d\tau'\{1/(2m)[p(\tau_b, \tau') - eA_l(\tau')]^2 + I_p\}$. The instant $\tau = \tau_r$ is obtained from stationary phase calculation of the Fourier integral of the atomic dipole moment and depends on N.

[11] C.-G. Wahlström *et al.*, Phys. Rev. A **48**, 4709 (1993); H. J. Shin, D. G. Lee, Y. H. Kyung, H. Hong, and C. H. Nam, Phys. Rev. Lett. **83**, 2544 (1999).

[12] C. H. Keitel and P. L. Knight, Phys. Rev. A **51**, 1420 (1995).